JACS
JOURNAL OF THE AMERICAN CHEMICAL SOCIETY
Article
pubs.acs.org/JACS

Lipid Bilayers Significantly Modulate Cross-Fibrillation of Two Distinct Amyloidogenic Peptides

Noga Gal,[†] Ahiud Morag,[†] Sofiya Kolusheva,[§] Roland Winter,[‡] Meytal Landau,[∥] and Raz Jelinek*[,†,§]

[†]Department of Chemistry, Ben Gurion University of the Negev, Beer Sheva, Israel 84105

[‡]Technische Universität Dortmund Physikalische Chemie – Biophysikalische Chemie, Otto-Hahn-Straße 6, 44227 Dortmund, Germany

[§]Ilse Katz Institute for Nanotechnology, Ben Gurion University Beer Sheva, Israel 84105

[∥]Department of Biology, Technion-Israel Institute of Technology, Haifa 32000, Israel

Supporting Information

ABSTRACT: Amyloid plaques comprising misfolded proteins are the hallmark of several incurable diseases, including Alzheimer's disease, type-II diabetes, Jacob–Creutzfeld disease, and others. While the exact molecular mechanisms underlying protein misfolding diseases are still unknown, several theories account for amyloid fiber formation and their toxic significance. Prominent among those is the "prion hypothesis" stipulating that misfolded protein seeds act as "infectious agents" propagating aggregation of nominally healthy, native proteins. Recent studies, in fact, have reported that interactions between different amyloid peptides that are partly sequence-related might also affect fibrillation pathways and pathogenicity. Here, we present evidence that two structurally and physiologically unrelated amyloidogenic peptides, the islet amyloid polypeptide (IAPP, the peptide comprising the amyloid aggregates in type II diabetes) and an amyloidogenic determinant of the prion protein (PrP), give rise to a significantly distinct fibrillation pathway when they are incubated together in the presence of membrane bilayers. In particular, the experimental data demonstrate that the lipid bilayer environment is instrumental in initiating and promoting the assembly of morphologically distinct fibrillar species. Moreover, cross-fibrillation produced peptide species exhibiting significantly altered membrane interaction profiles, as compared to the scenario where the two peptides aggregated separately. Overall, our data demonstrate that membranes constitute a critical surface-active medium for promoting interactions between disparate amyloidogenic peptides, modulating both fibrillation pathways as well as the biophysical properties of the peptide aggregates. This work hints that membrane-induced cross-fibrillation of unrelated amyloidogenic peptides might play an insidious role in the molecular pathologies of protein misfolding diseases.

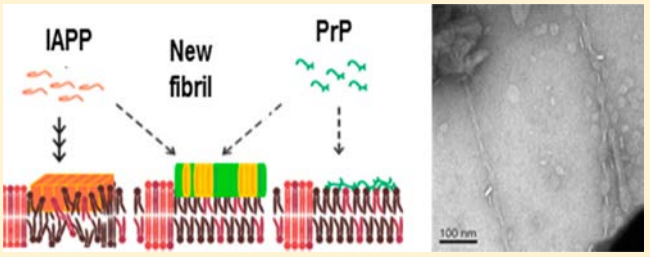

INTRODUCTION

Protein misfolding diseases, including Alzheimer's disease, type II diabetes, and prion diseases, encompass diverse pathologies, which, although varied in their physiological and medical manifestations, share a common trait, formation of insoluble aggregates comprising proteins and peptides that do not fold properly.[1] Indeed, numerous studies have revealed that different proteins that share little or no structural or sequence homologies form aggregates, sometimes referred to as amyloid plaques, comprising fibers that are remarkably similar in morphology, characterized by intermolecular antiparallel β-sheets, oriented roughly perpendicular to the axis of the fibers.[1]

Extensive research over the past several years has aimed to decipher the molecular basis of amyloid diseases.[2−4] However, there is still no concrete understanding of the factors responsible for the physiological characteristics and severe toxicity associated with such diseases. In particular, the relationship between protein fibrillation, on the one hand, disease initiation, and progression, on the other hand, has not been elucidated. Fibrillogenesis is believed to occur through nucleation–growth mechanisms in which monomeric amyloidogenic proteins assemble into long-range ordered fibers and plaques.[5,6] In this context, the "prion hypothesis", suggesting that misfolded protein species constitute "aggregation seeds" that promote further aggregation of native proteins, has established a specific molecular link between protein aggregation and disease.[7,8] Importantly, the prion hypothesis underscores the significance of protein–protein interactions in amyloidogenesis.[9]

While most previous investigations have focused on individual disease-specific peptides forming fibrillar aggregates (for example, aggregation of amyloid-beta (Aβ), the peptide constituent of the amyloid plaques associated with Alzheimer's disease[10]), recent studies have demonstrated that interactions between peptides associated with different diseases, respec-

Received: July 10, 2013
Published: August 16, 2013

   dx.doi.org/10.1021/ja4070427 | J. Am. Chem. Soc. 2013, 135, 13582–13589

tively, can modulate fibrillation pathways and impact cells in distinct manners as compared to the effects of the separate peptides.[11] For example, islet amyloid polypeptide (IAPP), associated with type-II diabetes,[12] and Aβ were found to interact and cross-fibrillate in vitro, which might account for the observation that patients with type II diabetics have a higher risk for contracting Alzheimer's disease and vice versa.[13] Cross fibrillation is probably related to the resemblance between IAPP and β-amyloid, which exhibit 25% sequence identity and 50% sequence similarity.[11]

In this work, we investigated the effects of interactions between IAPP and the 21-residue amyloidogenic determinant of the prion protein [PrP(106−126)][14] upon their fibrillation pathways and the biophysical properties of the resultant aggregate species. In particular, we aimed to evaluate peptide interactions and cross-fibrillation phenomena in the presence of membrane bilayers. Indeed, membranes and membrane interactions have emerged in recent years as fundamental factors involved in amyloidogenesis and protein fibrillation.[15] Numerous studies underscored the contributions and participation of lipid bilayers in protein misfolding processes, including the formation of amyloid peptide-induced pores and ion channels in membranes,[16] lipid-promoted fibrillation,[16] membrane-induced inhibition of amyloidogenesis,[16] and membranes as targets for docking of amyloid protein aggregates.[17]

MATERIALS AND METHODS

Materials. PrP(106−126) was purchased from Peptron (South Korea) in a lyophilized form at >90% purity (HPLC). Human IAPP (amylin, human) was obtained from Mercury (Rosh Haayin, Israel), L-α-phosphatidylcholine (egg, chicken), L-α-phosphatidylglycerol (egg, chicken) (sodium salt), 1,2-dimyristoyl-*sn*-glycero-3-phosphocholine (DMPC), 1,2-dimyristoyl-*sn*-glycero-3-[phospho-*rac*-(1-glycerol)] (DMPG), 1,2-dimyristoyl-*sn*-glycero-3-phosphoethanolamine-*N*-(7-nitro-2-1,3-benzoxadiazol-4-yl) (N-NBD-PE), and 1,2-dimyristoyl-*sn*-glycero-3-phosphoethanolamine-*N*-(lissamine rhodamine B sulfonyl) (N-Rh-PE) were purchased from Avanti Polar Lipids (AL). Thioflavin T (ThT), 1,1,1,3,3,3-hexafluoro-2-propanol, sodium hydrosulfite, and sodium phosphate monobasic were purchased from Sigma- Aldrich (Rehovot, Israel).

Peptide Sample Preparation. IAPP and PrP(106−126) were dissolved in 1,1,1,3,3,3-hexafluoroisopropanol (HFIP). IAPP was kept at a concentration of 0.5 mg/mL and PrP at 2.5 mM. The peptides were stored in these conditions at −20 °C until use to prevent fibril formation. For each experiment, the solution was thawed, and the required amount was dried by evaporation for 6−7 h to remove the HFIP. The dried peptide samples were dissolved in buffer consisting of 10 mM NaH_2PO_4, pH 7.5, at room temperature.

Thioflavin T (ThT) Fibrillation Assay. ThT fluorescence measurements were conducted at 25 °C on a Varioskan (Thermo, Finland), by using 96-well-plate path cell culture plates. ThT concentrations of 7.5 mM were used in 192 μL solutions in each well. Measurements of samples containing IAPP (15 μM), PrP (50 μM), and mixtures of both peptides, with lipid vesicles (final concentration 0.625 mM) and without vesicles present (both experiment were conducted in buffer consisting of 10 mM NaH_2PO_4, pH 7.5, kept at room temperature, liposomes were prepared using the same buffer), were conducted simultaneously to attain experimentally reliable comparisons. The device was programmed to record fluorescence intensity every minute for the initial 4 h and every 30 min for the remaining 20 h. Excitation and emission wavelengths were 440 and 485 nm, respectively. The fluorescence curves were smoothed by using a five-point adjacent averaging.

Förster Resonance Energy Transfer (FRET). Small unilamellar vesicles (SUVs) (DMPC/DMPG at 1:1 mol ratio) were prepared by dissolving the lipid components in chloroform/ethanol and drying together in vacuo, followed by dissolution in phosphate buffer (pH 7.5) by probe-sonication of the aqueous lipid mixture at room temperature for 10 min. Prior to drying, the lipid vesicles were additionally supplemented with 1,2-dimyristoyl-*sn*-glycero-3-phosphoethanolamine-*N*-(7-nitro-2-1,3-benzoxadiazol-4-yl (N-NBD-PE) and 1,2-dimyristoyl-*sn*-glycero-3-phosphoethanolamine-*N*-(lissamine rhodamine B sulfonyl) (N-Rh-PE) at a 500:1:1 mole ratio (phospholipid:N-NBD-PE:N-Rh-PE). IAPP (15 μM), PrP(106−126) (50 μM), and a mixture of both were added to the vesicles (final concentration 0.625 mM) at $t = 0$. Fluorescence emission spectra were acquired every 30 min for 12 h (excitation 469 nm) in the range of 490−650 nm using a Varioskan 96-well plate (Thermo, Finland).

To calculate the extent of FRET efficiency, the following equation was used:

$$\text{efficiency} = \frac{R_i - R_{100\%}}{R_0 - R_{100\%}} \times 100\%$$

in which R is a ratio of fluorescence emissions NBD-PE (536 nm)/Rhodamine B-PE (586 nm). R_i is the ratio in the peptide/vesicles mixtures, $R_{100\%}$ was measured following the addition of 20% Triton X-100 to the vesicles (Triton X-100 is a detergent causing complete dissolution of the vesicles), and R_0 corresponds to the ratio recorded for vesicles without any additives.

Fluorescence Quenching. SUVs were prepared according to the procedure above (FRET experiments). Prior to drying, the lipid vesicles were additionally supplemented with N-NBD-PE at a mole ratio of 1:100 (N-NBD-PE: total phospholipids). IAPP (15 μM), PrP(106−126) (50 μM), and a mixture of both peptides were added to the vesicles (final concentration 0.625 mM), and aliquots of 30 μL were diluted at specific time points in phosphate buffer (pH 7.5) to a final volume of 0.5 mL. The quenching reaction was initiated by adding sodium dithionite, from a stock solution of 0.6 M in 50 mM Tris buffer (pH 11), to give a final concentration of 1 mM. The decrease in fluorescence emission was recorded for 10 min at room temperature using 469 nm excitation and 560 nm emission on an FL920 spectrofluorimeter (Edinburgh, Scotland, UK). The fluorescence decay curves were calculated as a percentage of the initial fluorescence measured before the addition of dithionite.

Isothermal Titration Calorimetry (ITC). For individual peptide measurements, we used an initial 0.2 mM peptide concentration. The peptide mixture contained 154 μM PrP(106−126) and 46 μM IAPP (mole ratio of 3.33:1). 170 μL sample volume was inserted into the Nano ITC low volume cell (TA Instruments, Newcastle, DE), and the syringe was filled with 50 μL of DMPC/DMPG 1:1 5 mM SUVs. After reaching equilibrium, injection of 2 μL aliquots was carried out every 3 min for a total of 75 min. The TA Nano Analyzer software was used for data analysis.

Differential Scanning Calorimetry (DSC). Multilamellar vesicle dispersions were prepared by dissolving DMPC/DMPG (1:1 mol ratio) in chloroform/ethanol (1:1) and drying in vacuo to constant weight, followed by addition of phosphate buffer (pH 7.5, final lipid concentration 2 mM). Glass beads were then added, and the sample was thoroughly shaken. DSC experiments were performed on a VP-DSC microcalorimeter (MicroCal, U.S.). Phosphate buffer (pH 7.5), IAPP (15 μM), PrP(106−126) (50 μM), and a mixture of both peptides were added to the vesicles (final concentration 0.625 mM), and heating scans were run at a rate of 60 °C/h. Data analysis was performed by the Microcal Origin 7.0 software.

Transmission Electron Microscopy (TEM). Peptide aliquots (5 μL) from samples used in the ThT experiments (after 24 h incubation) were placed on 400-mesh copper grids covered with a carbon-stabilized Formvar film. Excess solutions were removed following 2 min of incubation, and the grids were negatively stained for 30 s with a 1% uranyl acetate solution. Samples were viewed in an FEI Tecnai 12 TWIN TEM operating at 120 kV.

RESULTS

This study examines the effect of lipid bilayers upon the fibrillation pathways of coincubated IAPP and PrP(106−126)

and the biophysical properties of the peptide aggregates. The vesicle system employed in the experiments was comprised of dimyristoylphosphatidylcholine (DMPC), a zwitterionic phospholipid, and dimyristoylphosphatidylglycerole (DMPG), which is negatively charged. This simple lipid combination is routinely used as a mimic for generic plasma membranes.[18] The presence of negatively charged lipids, in particular, has been widely shown to participate in peptide fibrillation phenomena.[19]

Figure 1 presents the time evolution of thioflavine-T (ThT) fluorescence emission, following addition of the dye to

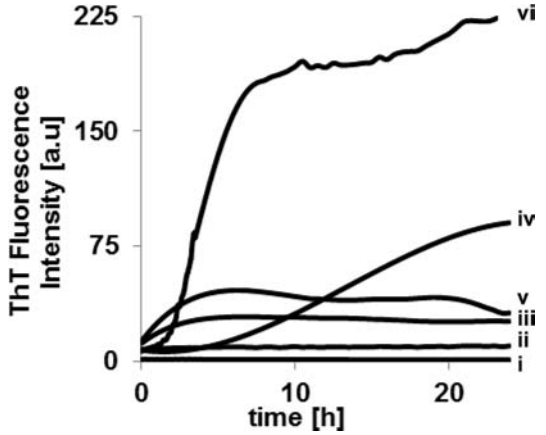

Figure 1. Kinetics of fiber formation. Time-dependent ThT fluorescence curves indicating dramatically enhanced fibrillation in a IAPP/PrP(106−126) mixture in the presence of DMPC/DMPG vesicles. (i) PrP(106−126) in buffer; (ii) PrP(106−126) in DMPC/DMPG vesicle suspension; (iii) IAPP in buffer; (iv) IAPP in DMPC/DMPG vesicle suspension; (v) IAPP+PrP(106−126) in buffer; (vi) IAPP+PrP(106−126) in DMPC/DMPG vesicle suspension.

solutions comprising the two peptides, with and without DMPC/DMPG vesicles present. ThT is a common marker for fiber formation as this small molecule fluoresces upon insertion into β-sheet fibrillar structures.[20,21] The ThT fluorescence curves in Figure 1 attest to enhanced fibrillation of PrP(106−126) and IAPP incubated separately with lipid bilayers in comparison with lipid-free solutions [Figure 1, curves i,ii (PrP) and iii,iv (IAPP)]. Membrane-induced fibrillation of amyloid peptides, including IAPP and PrP, have been previously reported.[22,23]

The ThT data in Figure 1, however, point to a dramatic fibrillation enhancement when PrP(106−126) and IAPP were mixed and then added to the DMPC/DMPG suspension. Indeed, the fluorescence emission ThT when added to the PrP(106−126) and IAPP together in the presence of the lipid vesicles (Figure 1, vi) was substantially higher in comparison with either the two peptides without lipids (Figure 1, v), but also as compared to the individual peptides incubated separately with the lipid vesicles (Figure 1, iv, ii). Additional ThT experiments underscore the prominent role of the negatively charged headgroup of the phospholipid in promoting the observed enhanced fibrillation. Supporting Information Figure S1, for example, reveals negligible fibrillation of the individual peptides or the peptide mixture in the presence of either zwitterionic or positively charged moieties, while pronounced fibrillation was recorded for PrP(106−126)/IAPP mixtures in the presence of vesicles containing dimyristoylphosphatidylserine (DMPS) or phosphatidic acid (PA); both exhibit negatively charged headgroups.

As the ThT fluorescence results in Figure 1 point to significant lipid-induced modulation of fiber formation in the IAPP and PrP(106−126) mixture, we next characterized the biophysical and structural properties of the peptide species assembled (Figures 2−5). Specifically, the experiments were

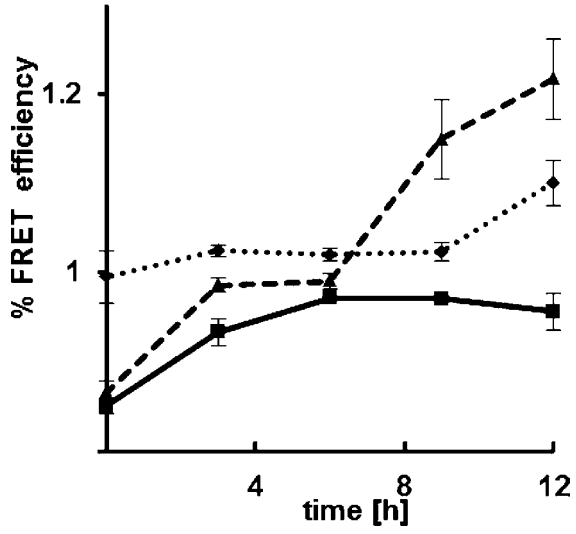

Figure 2. Modulation of bilayer properties induced by peptide aggregation. Förster resonance energy transfer (FRET) between NBD-PE and Rh-PE dyes embedded within DMPC/DMPG bilayer vesicles. FRET was recorded at different time-points after peptide dissolution in the vesicle solution. Solid line, IAPP alone; dotted line, PrP(106−126); dashed line, IAPP/PrP mixture. Value of "1" corresponds to FRET in the control vesicles (no peptides added).

designed to assess whether the interactions between IAPP and PrP(106−126) affected membrane interactions of the aggregates formed. Close interplay between membrane interactions and aggregation pathways of amyloidogenic peptides has been observed in many instances.[24] In particular, oligomeric and prefibrillar species formed in the initial stages of peptide fibrillation pathways have been shown to exhibit significant interactions with lipid bilayers.[25,26]

Figure 2 depicts Förster resonance energy transfer (FRET) results recorded upon incubation of the peptides with DMPC/DMPG vesicles that also contained NBD-PE (fluorescence energy donor) and Rh-PE (fluorescence acceptor). Modulation of the fluorescence energy transferred between the donor and acceptor embedded within lipid bilayers is a sensitive probe for the effect of membrane-active species upon lipid bilayers.[27] Specifically, lipid reorganization and bilayer fluidity changes induced by amphiphilic or hydrophobic substances have been shown to modulate the FRET between membrane-embedded dyes.[22,28,29] In the context of this work, FRET experiments have been previously applied for evaluating bilayer interactions of amyloidogenic peptides.[22,30]

The FRET time evolutions recorded in NBD-PE/Rh-PE/DMPC/DMPG vesicles (1:1:500:500 molar ratio) depicted in Figure 2 indicate that the IAPP/PrP(106−126) mixture exerted a distinct impact upon lipid bilayers as compared to the effects of the individual peptides incubated separately with the vesicles. Specifically, incubation of IAPP alone with the NBD-PE/Rh-PE/DMPC/DMPG vesicles gave rise to lower energy transfer as compared to the control vesicles. This effect was apparent in

dx.doi.org/10.1021/ja4070427 | J. Am. Chem. Soc. 2013, 135, 13582−13589

all time-points recorded (Figure 2, solid line). This result reflects disruption of the bilayer by the peptide, leading to less efficient energy transfer.[31] PrP(106−126) alone affected the FRET differently (Figure 2, dotted line). Essentially, this peptide had a negligible effect upon the FRET between the vesicle-embedded donors and acceptors except for the last time point, in which the prion fragment increased FRET efficiency, indicating a different bilayer binding mechanism as compared to IAPP.[22]

The IAPP/PrP(106−126) mixture, however, gave rise to a significantly different FRET time evolution as compared to the two peptides added separately (Figure 2, long dash). Initially, the peptide mixture induced lesser FRET upon addition to the NBD-PE/Rh-PE/DMPC/DMPG vesicles, similar to IAPP alone. However, the FRET efficiency considerably increased in subsequent time-points, ultimately giving rise to much higher FRET efficiency, both as compared to the control vesicles (with no peptides added), as well as in comparison with the two peptides added separately. The enhanced FRET is due to closer average distance between the membrane-embedded dyes and likely reflects a distinct bilayer interaction of the aggregates formed through coincubation of IAPP and PrP(106−126), possibly also invoking formation of mixed lipid-peptide assemblies.

The fluorescence quenching experiments presented in Figure 3 corroborate the FRET results and their interpretation. In fluorescence quenching experiments, sodium dithionite is added to vesicles incorporating the fluorescent dye NBD-PE, resulting in gradual quenching of the fluorescence emission of the dye.[32] Importantly, the NBD quenching curves are highly sensitive to addition of membrane-active species, which modulate the interactions between the dithionite quencher and the bilayer-embedded fluorescent dye.[29] This observation makes fluorescence quenching analysis a useful tool for evaluating membrane interactions and subsequent bilayer reorganization.

Figure 3 demonstrates significantly different effects upon the NBD quenching curves by IAPP alone, PrP(106−126) alone, and the two peptides coincubated with the NBD-PE/DMPC/DMPG vesicles. In the case of IAPP (Figure 3), at the two incubation times examined (short time after addition of the peptide to the vesicles, and after 12 h incubation), the peptide gave rise to more pronounced fluorescence quenching. This result is indicative of bilayer perturbations by the peptide and/or its aggregates, leading to excess exposure of the bilayer-embedded NBD dye and subsequently to enhanced quenching by the dithionite.[32] This scenario is consistent with the FRET data in Figure 2, which also point to a considerable degree of bilayer reorganization occurring in parallel with the IAPP fibrillation process.

In contrast to IAPP, PrP(106−126) impeded dithionite-induced NBD quenching, particularly after 12 h incubation (Figure 3). This result is likely ascribed to bilayer "shielding" by the assembled PrP(106−126) fibers, a phenomenon reported previously in the case of PrP and other fibrillar peptides.[16] The fluorescence quenching data acquired following incubation of the NBD-PE/DMPC/DMPG vesicles with IAPP and PrP(106−126) together (Figure 3) are different from either IAPP by itself or PrP(106−126). Specifically, a significantly faster quenching rate was observed a short time after addition of the peptide mixture to the vesicles (Figure 3, dotted curve), a result that is very similar to the quenching rate recorded following addition of IAPP alone (Figure 3, dotted curve).

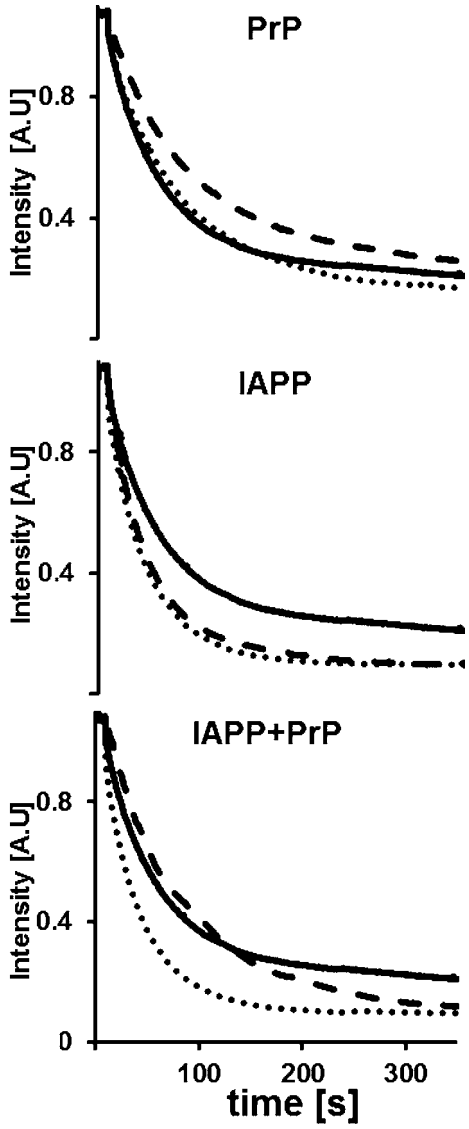

Figure 3. Fluorescence quenching. Fluorescence quenching curves of NBD-PE embedded in DMPC/DMPG vesicles following addition of sodium dithionate at t = 0. The vesicles were incubated with PrP, IAPP, or their mixture. Measurements were carried out immediately after peptide addition (dotted curves) or after 12 h of incubation (long dash). The bold curves correspond to the control vesicles (without coaddition of peptides). Different effects of the peptides upon bilayer organization are apparent.

However, the fluorescence quenching curve recorded after 12 h of incubation is close to the control curve (Figure 3, broken curve), indicating less pronounced bilayer disruption. This result is consistent with the FRET data in Figure 2 and similarly points to a distinct mechanism of bilayer interaction by the peptide species formed through coincubation of the two peptides.

To further illuminate the binding of the individual peptides and peptide mixture to the DMPC/DMPG vesicles, we carried out isothermal titration calorimetry (ITC) experiments, designed to probe the thermodynamic parameters pertaining to the peptide-lipid binding events[33] (Figure 4). Consistent with, and complementing the quenching and FRET data presented above, the ITC results point to pronounced

dx.doi.org/10.1021/ja4070427 | J. Am. Chem. Soc. 2013, 135, 13582−13589

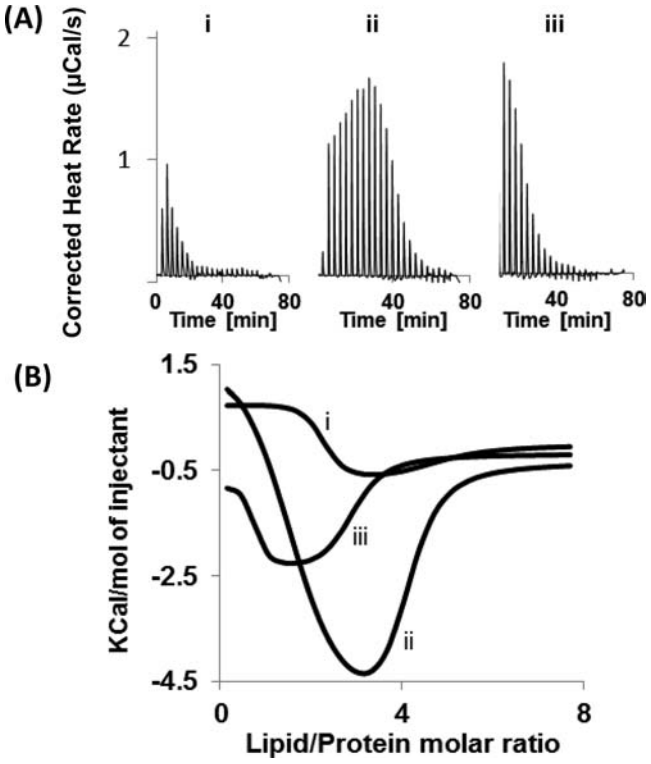

Figure 4. Binding of the peptides to lipid bilayers. Isothermal titration calorimetry (ITC) data recorded upon addition of DMPC/DMPG vesicles to (i) PrP(106−126); (ii) IAPP; (iii) PrP(106−126) + IAPP mixture. (A) Heat flows recorded after injection of 2 μL vesicle aliquots. (B) Molar heat values obtained through integration of the individual heat flow signals, as a function of total lipid/peptide mole ratio. The titration isotherm data points to distinct vesicle binding mechanism of the peptide mixture.

differences in the vesicle binding profile of the PrP/IAPP mixture, as compared to the two peptides added separately.

The raw ITC heat trace data in Figure 4A demonstrate significant differences in the exothermic enthalpy released in the titration process among the three samples, PrP(106−126) and IAPP individually (Figure 4A,i and 4A,ii, respectively) and the PrP(106−126)/IAPP mixture (Figure 4A,iii). The distinct binding mechanism of the peptide mixture is particularly apparent in Figure 4B, depicting the binding isotherms calculated through integration of the titration peaks in Figure 4A for each peptide sample.

Notably, the binding isotherm of the peptide mixture (Figure 4B, curve iii) does not reflect superimposition (nor subtraction) of the isotherms calculated for titrations of the two peptides separately (Figure 4B, i and ii). This observation is important, because it indicates that binding of the species formed in the peptide mixture exhibits a unique bilayer binding mechanism (reflecting distinct affinity, enthalpy, and stoichiometry of the binding reaction) that is significantly different from the binding profiles of the two amyloid peptides added individually to the vesicles.

While the ITC analysis in Figure 4 underscores the distinct binding mechanism of the IAPP-PrP(106−126)/IAPP peptide mixture, we applied differential scanning calorimetry (DSC) experiments to probe the effect of peptide binding upon lipid organization within the bilayer (Figure 6). DSC is a sensitive technique for deciphering changes in organization and cooperative properties of lipid bilayers.[34] The technique has been particularly useful to probe membrane interactions of amyloidogenic peptides.[35]

Consistent with the experiments discussed above, the DSC results in Figure 5 point to a dramatically different bilayer

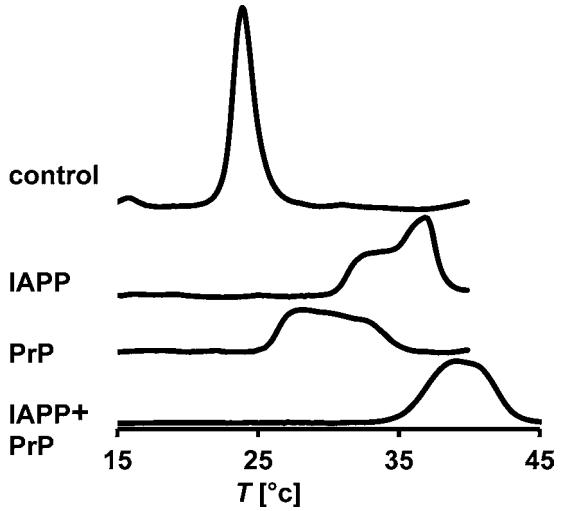

Figure 5. Effect of peptide aggregation upon thermodynamic properties of the lipid bilayers. Differential scanning calorimetry (DSC) thermograms of DMPC/DMPG vesicles incubated with IAPP alone, PrP(106−126) alone, or IAPP/PrP(106−126) mixture, respectively. The substantial temperature shifts and broadening of the phase transition are indicative of a modulation of the bilayer organization induced by the peptide aggregates formed during the fibrillation process.

reorganization induced by the fibrillar species formed in the IAPP/PrP(106−126) mixture, as compared to the effect of each peptide separately. Specifically, while the thermogram of the control DMPC/DMPG vesicles exhibits the expected single gel-to-fluid phase transition at 24 °C,[34,36] incubation of the vesicles with the amyloidogenic peptides significantly increased the temperature and broadened the phase transition (Figure 5), indicating phase separation into regions of different lateral organization. The pronounced changes of the lipid phase transition are a consequence of strong interactions with the peptide's aggregate structures, which significantly alter the lipid bilayer organization and interfere with the cooperative transition of the lipid acyl chains.[35]

Of particular significance in the DSC results in Figure 5 is the pronounced effect of the IAPP/PrP(106−126) mixture upon the cooperative thermal transition of the lipid bilayer. Indeed, the mixture induced a significantly greater temperature shift as compared to incubation of the peptides separately. Consistent with the FRET and quenching data discussed above, this result likely underscores a distinct membrane binding and bilayer disruption mechanism associated with the lipid-induced fibrillar species formed in the IAPP/PrP(106−126) mixture, as compared to the two peptides incubated separately.

As discussed above, Figures 2−5 show that peptide species formed during cross-fibrillation within the IAPP/PrP(106−126) mixture exhibit distinct membrane interaction profiles, clearly different from the individual peptides. A crucial question, however, is whether the fibers formed in the peptide mixture incubated with the lipid vesicles adopt distinct structural features. Indeed, the representative TEM images in Figure 6 provide dramatic visual depictions of the different fiber

dx.doi.org/10.1021/ja4070427 | J. Am. Chem. Soc. 2013, 135, 13582−13589

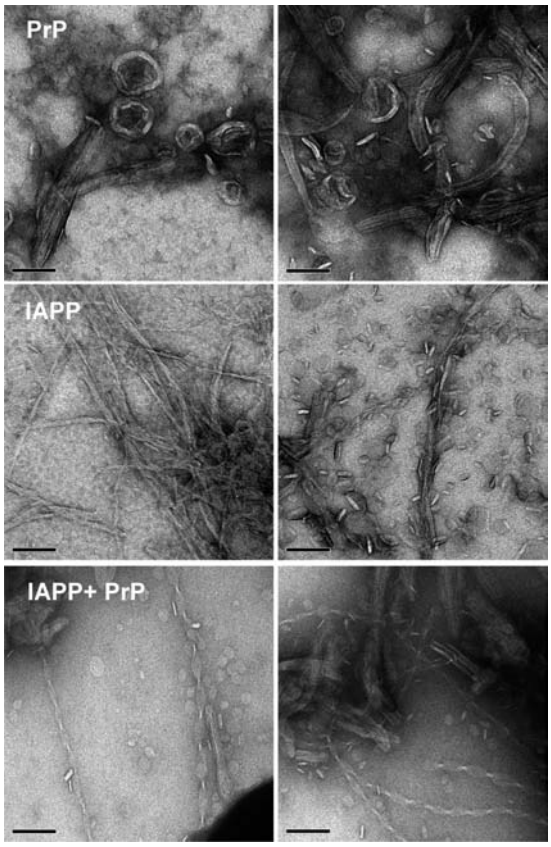

Figure 6. Peptide-assembled fiber morphologies. Transmission electron microscopy (TEM) images recorded from lipid vesicle solutions of the peptides. Each row depicts two representative images. Scale bars in all images correspond to 100 nm.

morphologies formed following incubation of the peptides in the DMPC/DMPG vesicle solutions. PrP(106−126) incubated separately with lipid bilayers formed thick, short fiber bundles,[5] which were closely associated with the vesicles (Figure 6, top images). When IAPP alone was incubated with the vesicles, it assembled into elongated thin fibers,[23] interspersed with abundant proto-fibrillar aggregates (Figure 6, middle).

Inspection of the IAPP/PrP(106−126) mixture, however, reveals an abundance of striking regularly twisted fibrillar structures (Figure 6, bottom images). The twisted structures were not observed in IAPP/PrP(106−126) mixture incubated in buffer (i.e., without vesicles). While screw-shaped fiber morphologies have been observed in protein aggregation phenomena,[39] this topology has not been reported for either IAPP or PrP. The observation of twisted fiber structures provides strong evidence for the coassembly of both peptides forming distinctly new fiber morphology.

■ DISCUSSION

Among the primary impetus for this study is the yet unexplained observation that patients inflicted with certain amyloid diseases have higher chances of acquiring unrelated protein misfolding diseases. In this context, this study aims to address an important, largely overlooked issue in protein fibrillation phenomena, particularly involving putative interactions between amyloid proteins. Specifically, the experiments were designed to determine whether the IAPP and PrP(106−126) peptides, which do not share structure and sequence homology and are associated with different diseases, interact with each other when incubated together in the presence of lipid bilayers. In particular, the underlying question addressed by this study is whether such interactions alter their fibrillation profiles and fiber properties.

The results presented clearly demonstrate that lipid vesicles intimately affect interactions between the two peptides, consequently modulating fibrillation pathways and the properties of the coassembled peptide aggregates. Interactions between different amyloidogenic peptides have been reported. "Cross-seeding" between bacterial amyloid curli peptides have been implicated in mixed-species biofilm formation.[40] "Cross-fibrillation" phenomena involving IAPP and amyloid-β have been recently reported.[11,12] These observations have been generally ascribed to the sequence similarity between these two peptides.[11,12] The experiments reported here, however, differ in a critical aspect from previous cross-fibrillation analyses due to the fact that the two peptides we studied, IAPP and PrP(106−126), do not share sequence identity or similarity.

A principal observation in this study is the crucial role of negatively charged lipid bilayers in promoting peptide interactions and modulating the fibrillation pathway. The ThT fluorescence data, in particular, point to a dramatic modulation of the fibrillation reaction when the peptide mixture is incubated in vesicle suspension as compared to an aqueous solution not containing lipid bilayers (Figure 1). The ThT results might be explained by either enhanced fibrillation and/or formation of different fibrillar structures. Both scenarios, however, directly depend on the presence of the DMPC/DMPG bilayer environment. While the exact nature and significance of membranes in amyloidogenesis and protein misfolding have not been elucidated yet, numerous reports have demonstrated the significance and close relationship between lipid membranes and peptide aggregation.[24,41,42] One possible explanation is that the membrane provides a platform that increases the local concentration of the two amyloidogenic peptides, thereby facilitating fiber nucleation.[43] This study further underscores the critical role of lipid membranes in sequestering amyloidogenic peptides and promoting "communication" and interactions between two distinct amyloidogenic peptides, thereby intimately modulating their fibrillation pathways and fibrillar morphologies.

A key question one needs to address is whether vesicle-induced interactions between IAPP and PrP(106−126) lead to the assembly of mixed fibrillar species, comprising both peptide molecules. This issue has significant physiological implications because assemblies formed through peptide aggregation processes, such as oligomers, proto-fibrils, and fibers, have been shown to impact the cellular membranes, likely interfering with their biological functioning and contributing to the toxic effects encountered in protein misfolding diseases.[7,9,44] The data presented here do not provide a conclusive answer to the above question; however, altogether the experiments strongly suggest that so far unknown unique aggregate species did indeed form from the peptide mixture.

Specifically, the biophysical techniques applied (Figure 2−5) clearly demonstrate that the fibrillation process goes hand in hand with distinct membrane interactions, which appear differently as compared to each peptide incubated separately with the vesicles. Indeed, the membrane interactions analyzed through the various biophysical techniques appear not as simple addition, "average", nor synergistic enhancement of the respective effects of the separate peptide species, but as being rather unique.

The TEM examination of the different fibrillar species (Figure 6) lends further support to the notion that coincubation of IAPP and PrP(106−126) in the presence of negatively charged lipid vesicles gives rise to distinct fibers comprising both peptides. Specifically, the remarkable screw-shaped fiber morphology recorded in the peptide mixture is markedly different from the fibrillar structures observed for the individual peptides. Indeed, fibril morphologies of IAPP and IAPP+PrP(106−126) incubated in buffer were highly similar to IAPP alone (Supporting Information Figure S4) [PrP(106−126) alone does not noticeably fibrillate within shorter time spans when vesicles are not present].

It should be also noted that the ratio between the two peptides in the mixture appears to be an important parameter contributing to cross-fibrillation and the intriguing morphology associated with the fibers. Indeed, it appears that the specific IAPP:PrP(106−126) mole ratio employed here is required for triggering cross fibrillation; when mixtures containing higher mole ratio between IAPP and PrP(106−126) were examined by electron microscopy, the images revealed a much higher abundance of IAPP-like fibrils (Supporting Information Figure S2).

While the exact mechanisms responsible for lipid-induced seeding, "cross fibrillation", and the resultant twisted morphology and distinct membrane interactions have not been fully established yet, the experiments suggest that the lipid bilayers, through the negatively charged moieties displayed on their surface, promote formation of aggregation nuclei.[45] We can speculate that such nuclei, comprising PrP(106−126), IAPP, or both, constitute a platform for further fibrillation that do not discriminate between the two peptides, resulting in the formation of mixed fibrils exhibiting the intriguing twisted morphology and unique biophysical properties. Indeed, the enhanced fibrillation of the PrP(106−126) + IAPP mixture as compared to the two peptides taken separately supports a basic cross-seeding effect, which amplifies the intrinsic aggregation tendency of the individual peptides.

In accordance with the experimental results, calculations of the amyloidogenic propensity of PrP and IAPP, using the 3D-profile method[46,47] (Supporting Information Figure S3), reveal that segments of PrP and IAPP show the propensity to interact and form short, self-complementing pairs of β-sheets termed steric zippers,[48] which could serve as a core of a mixed fiber assembly.

In conclusion, this work reveals a critical role of negatively charged lipid membrane environments in promoting mutual interactions between different amyloidogenic peptides, resulting in unique fibrillation phenomena and distinct biophysical properties of the assembled peptide species. Membrane-promoted cross-fibrillation between unrelated peptides might play a prominent role in the spread of amyloidogenic diseases and point to previously unrecognized pathological pathways in protein misfolding diseases.

■ ASSOCIATED CONTENT

Supporting Information

ThT fluorescence curves of the peptides in the presence of zwitterionic, positively charged, and negatively charged lipids, respectively. TEM images of fibers formed in vesicle solutions containing the PrP(106−126)/IAPP mixture in a lower mole ratio (e.g., higher IAPP concentration). Amyloidogenic propensity of IAPP and PrP(106−126) homotypic and heterotypic interactions predicted by the 3D-profile method. This material is available free of charge via the Internet at http://pubs.acs.org.

■ AUTHOR INFORMATION

Corresponding Author

razj@bgu.ac.il

Notes

The authors declare no competing financial interest.

■ ACKNOWLEDGMENTS

We are grateful to Dr. Lukasz Goldschmit, UCLA, for carrying out the calculations.

■ REFERENCES

(1) Harrison, R. S.; Sharpe, P. C.; Singh, Y.; Fairlie, D. P. *Rev. Physiol. Biochem. Pharmacol.* **2007**, *159*, 1−77.
(2) Kepp, K. P. *Chem. Rev.* **2012**, *112*, 5193−239.
(3) Stefani, M. *Prog. Neurobiol.* **2012**, *99*, 226−45.
(4) Olzscha, H.; Schermann, S. M.; Woerner, A. C.; Pinkert, S.; Hecht, M. H.; Tartaglia, G. G.; Vendruscolo, M.; Hayer-Hartl, M.; Hartl, F. U.; Vabulas, R. M. *Cell* **2011**, *144*, 67−78.
(5) Bazar, E.; Jelinek, R. *ChemBioChem* **2010**, *11*, 1997−2002.
(6) Svane, A. S. P.; Jahn, K.; Deva, T.; Malmendal, A.; Otzen, D. E.; Dittmer, J.; Nielsen, N. C. *Biophys. J.* **2008**, *95*, 366−77.
(7) Cashman, N. R.; Caughey, B. *Nat. Rev. Drug Discovery* **2004**, *3*, 874−84.
(8) Rehders, D.; Claasen, B.; Redecke, L.; Buschke, A.; Reibe, C.; Jehmlich, N.; Von Bergen, M.; Betzel, C.; Meyer, B. *J. Mol. Biol.* **2009**, *392*, 198−207.
(9) Cobb, N. J.; Surewicz, W. K. *Biochemistry* **2009**, *48*, 2574−85.
(10) Straub, J.; Guevara, J. *Acc. Chem. Res.* **2002**, *35*, 473−481.
(11) O'Nuallain, B.; Williams, A. D.; Westermark, P.; Wetzel, R. *J. Biol. Chem.* **2004**, *279*, 17490−9.
(12) Seeliger, J.; Evers, F.; Jeworrek, C.; Kapoor, S.; Weise, K.; Andreetto, E.; Tolan, M.; Kapurniotu, A.; Winter, R. *Angew. Chem., Int. Ed.* **2012**, *51*, 679−83.
(13) Nicolls, M. *Curr. Alzheimer Res.* **2004**, *1*, 47−54.
(14) Tagliavini, F.; Prelli, F.; Verga, L.; Giaccone, G.; Sarma, R.; Gorevic, P.; Ghetti, B.; Passerini, F.; Ghibaudi, E.; Forloni, G. *Proc. Natl. Acad. Sci. U.S.A.* **1993**, *90*, 9678−82.
(15) Jelinek, R.; Sheynis, T. *Curr. Protein Pept. Sci.* **2010**, 372−384.
(16) Sheynis, T.; Jelinek, R. *J. Phys. Chem. B* **2010**, *114*, 15530−5.
(17) Bucciantini, M.; Cecchi, C. *Methods Mol. Biol.* **2010**, *648*, 231−43.
(18) Chakraborty, H.; Sarkar, M. *Biophys. Chem.* **2007**, *125*, 306−13.
(19) Sellin, D.; Yan, L.-M.; Kapurniotu, A.; Winter, R. *Biophys. Chem.* **2010**, *150*, 73−9.
(20) Krebs, M. R. H.; Bromley, E. H. C.; Donald, A. M. *J. Struct. Biol.* **2005**, *149*, 30−7.
(21) Biancalana, M.; Koide, S. *Biochim. Biophys. Acta* **2010**, *1804*, 1405−1412.
(22) Bazar, E.; Sheynis, T.; Dorosz, J.; Jelinek, R. *ChemBioChem* **2011**, *12*, 761−7.
(23) Porat, Y.; Kolusheva, S.; Jelinek, R.; Gazit, E. *Biochemistry* **2003**, *42*, 10971−10977.
(24) Jayasinghe, S. A.; Langen, R. *Biochemistry* **2005**, *44*, 12113−9.
(25) Xue, W.; Hellewell, A.; Hewitt, E.; Radford, S. *Prion* **2010**, *4*, 20−25.
(26) Bucciantini, M.; Calloni, G.; Chiti, F.; Formigli, L.; Nosi, D.; Dobson, C. M.; Stefani, M. *J. Biol. Chem.* **2004**, *279*, 31374−82.
(27) Loura, L. M. S.; Rodrigo, F. M.; de Almeida, M. P. *J. Fluoresc.* **2001**, *11*, 197−209.
(28) Gal, N.; Malferarri, D.; Kolusheva, S.; Galletti, P.; Tagliavini, E.; Jelinek, R. *Biochim. Biophys. Acta* **2012**, *1818*, 2967−74.
(29) Gal, N.; Kolusheva, S.; Kedei, N.; Telek, A.; Naeem, T. A.; Lewin, N. E.; Lim, L.; Mannan, P.; Garfield, S. H.; El Kazzouli, S.;

Sigano, D. M.; Marquez, V. E.; Blumberg, P. M.; Jelinek, R. *ChemBioChem* **2011**, *12*, 2331−2340.
(30) Shtainfeld, A.; Sheynis, T.; Jelinek, R. *Biochemistry* **2010**, *49*, 5299−307.
(31) Loura, L. M. S.; Prieto, M. *Front. Physiol.* **2011**, *2*, 82.
(32) McIntyre, J. C.; Sleight, R. G. *Biochemistry* **1991**, *30*, 11819−27.
(33) Anbazhagan, V.; Sankhala, R. S.; Singh, B. P.; Swamy, M. J. *PloS One* **2011**, *6*, e25993.
(34) McElhaney, R. *Chem. Phys. Lipids* **1982**, *30*, 229−259.
(35) Del Mar Martínez-Senac, M.; Villalaín, J.; Gómez-Fernández, J. C. *Eur. J. Biochem.* **1999**, *265*, 744−53.
(36) Chapman, D.; Urbina, J.; Keough, K. *J. Biol. Chem.* **1974**, 249.
(37) Tenidis, K.; Waldner, M.; Bernhagen, J.; Fischle, W.; Bergmann, M.; Weber, M.; Merkle, M. L.; Voelter, W.; Brunner, H.; Kapurniotu, A. *J. Mol. Biol.* **2000**, *295*, 1055−71.
(38) Azriel, R.; Gazit, E. *J. Biol. Chem.* **2001**, *276*, 34156−61.
(39) Pashuck, E. T.; Stupp, S. I. *J. Am. Chem. Soc.* **2010**, *132*, 8819−21.
(40) Zhou, Y.; Smith, D.; Leong, B. J.; Brännström, K.; Almqvist, F.; Chapman, M. R. *J. Biol. Chem.* **2012**, *287*, 35092−103.
(41) Murray, I.; Sindoni, M.; Axelsen, P. *Biochemistry* **2005**, 12606−12613.
(42) Sciacca, M. F. M.; Brender, J. R.; Lee, D.-K.; Ramamoorthy, A. *Biochemistry* **2012**, *51*, 7676−84.
(43) Rhoades, E.; Agarwal, J.; Gafni, A. *Biochim. Biophys. Acta* **2000**, *1476*, 230−8.
(44) Broadley, S. A.; Hartl, F. U. *FEBS Lett.* **2009**, *583*, 2647−53.
(45) Sparr, E.; Engel, M. F. M.; Sakharov, D. V.; Sprong, M.; Jacobs, J.; De Kruijff, B.; Höppener, J. W. M.; Killian, J. A. *FEBS Lett.* **2004**, *577*, 117−20.
(46) Goldschmidt, L.; Teng, P. K.; Riek, R.; Eisenberg, D. *Proc. Natl. Acad. Sci. U.S.A.* **2010**, *107*, 3487−92.
(47) Thompson, M. J.; Sievers, S. A.; Karanicolas, J.; Ivanova, M. I.; Baker, D.; Eisenberg, D. *Proc. Natl. Acad. Sci. U.S.A.* **2006**, *103*, 4074−8.
(48) Sawaya, M. R.; Sambashivan, S.; Nelson, R.; Ivanova, M. I.; Sievers, S. A.; Apostol, M. I.; Thompson, M. J.; Balbirnie, M.; Wiltzius, J. J. W.; McFarlane, H. T.; Madsen, A. Ø.; Riekel, C.; Eisenberg, D. *Nature* **2007**, *447*, 453−7.